Quaternary Research 75 (2011) 183–195

Contents lists available at ScienceDirect

Quaternary Research

journal homepage: www.elsevier.com/locate/yqres

Timing of glaciation and last glacial maximum paleoclimate estimates from the Fish Lake Plateau, Utah

David W. Marchetti [a,*], M. Scott Harris [b], Christopher M. Bailey [c], Thure E. Cerling [d], Sarah Bergman [e]

[a] Geology Program, Western State College of Colorado, 600 N. Adams St. Gunnison, CO 81230, USA
[b] Department of Geology and Environmental Sciences, College of Charleston, 66 George St. Charleston, SC 29424, USA
[c] Department of Geology, College of William and Mary, 251 Jamestown Road, Williamsburg, VA 23185, USA
[d] Department of Geology and Geophysics, University of Utah, 115 S. 1460 E. Room 383, Salt lake City, UT 84112, USA
[e] Department of Geology, Carleton College, One North College Street, Northfield, MN 55057, USA

ARTICLE INFO

Article history:
Received 3 March 2010
Available online 15 October 2010

Keywords:
Alpine glaciation
Cosmogenic exposure-age dating
Colorado Plateau
Western U.S.

ABSTRACT

The High Plateaus of Utah include seven separate mountain ranges that supported glaciers during the Pleistocene. The Fish Lake Plateau, located on the eastern edge of the High Plateaus, preserves evidence of at least two glacial advances. Four cosmogenic ^{3}He exposure ages of boulders in an older moraine range from 79 to 159 ka with a mean age of 129 ± 39 ka and oldest ages of 152 ± 3 and 159 ± 5 ka. These ages suggest deposition during the type Bull Lake glaciation and Marine Oxygen Isotope Stage (MIS) 6. Twenty boulder exposure ages from four different younger moraines indicate a local last glacial maximum (LGM) of ~21.1 ka, coincident with the type Pinedale glaciation and MIS 2. Reconstructed Pinedale-age glaciers from the Fish Lake Plateau have equilibrium-line altitudes ranging from 2950 to 3190 m. LGM summer temperature depressions for the Fish Lake Plateau range from −10.7 to −8.2°C, assuming no change in precipitation. Comparison of the Fish Lake summer temperature depressions to a regional dataset suggests that the Fish Lake Plateau may have had a slight increase (~1.5× modern) in precipitation during the LGM. A series of submerged ridges in Fish Lake were identified during a bathymetric survey and are likely Bull Lake age moraines.

Introduction

Determining the timing of mountain glacier advance and its paleoclimatic and geomorphic significance has long been a major focus in Quaternary research (e.g. Thackray et al., 2008; Owen et al., 2009). In the past decade, several studies have documented significant variability in the timing and magnitude of Quaternary glaciations around the western U.S. (Owen et al., 2003; Licciardi et al., 2004; Benson et al., 2005; Laabs et al., 2006; Munroe et al., 2006; Licciardi and Pierce, 2008; Laabs et al., 2009). These records inform our still incomplete understanding of the synoptic-scale response of paleoglaciers to climate changes during and after the global last glacial maximum (LGM) (Clark et al., 2009). Several records also include data for the even more poorly resolved penultimate glaciation (e.g. Phillips et al., 1997; Easterbrook et al., 2003; Sharp et al., 2003; Licciardi and Pierce, 2008). Despite these studies, more data are required to improve our understanding of the regional response of glaciers to the last and prior deglaciations in the western U.S. Additionally, more records are needed from locations that can test hypotheses regarding the possible influence of the Laurentide ice sheet on continental scale atmospheric circulation affecting glacial mass balance (e.g. Bartlein et al., 1998; Thackray et al., 2004; Thackray, 2008) and the possible effect of pluvial lakes on localized lake-enhanced snowfall affecting glacial timing and magnitude (McCoy and Williams, 1985; Hostetler et al., 1994; Munroe et al., 2006; Laabs et al., 2009). One location that has several formerly glaciated ranges that span a wide range of latitude and may provide insight into both of those questions is the High Plateaus of Utah.

The High Plateaus of Utah are one of the most prominent geographic features in the state of Utah, and define the structural and geothermal transition between the Basin and Range and Colorado Plateau physiographic provinces (Wannamaker et al., 2001) (Fig. 1). Many of the higher elevation areas of the High Plateaus were glaciated during the Pleistocene (Marchetti, 2007). The Wasatch Plateau (Spieker and Billings, 1940), Fish Lake Plateau (Dutton, 1880; Hardy and Muessig, 1952; Osborn and Bevis, 2001), Aquarius Plateau–Boulder Mountain (Flint and Denny, 1958; Osborn and Bevis, 2001; Marchetti et al., 2005,2007), Markagunt Plateau (Mulvey et al., 1984; Currey et al., 1986), Tushar Mountains (Mulvey, 1985; Osborn and Bevis, 2001), northern Sevier Plateau (Osborn and Bevis, 2001; Jones et al, 2009) and Pavant Range (Mulvey, 1985; Oviatt, 1992; Osborn

* Corresponding author.
E-mail address: dmarchetti@western.edu (D.W. Marchetti).

0033-5894/$ – see front matter © 2010 University of Washington. Published by Elsevier Inc. All rights reserved.
doi:10.1016/j.yqres.2010.09.009

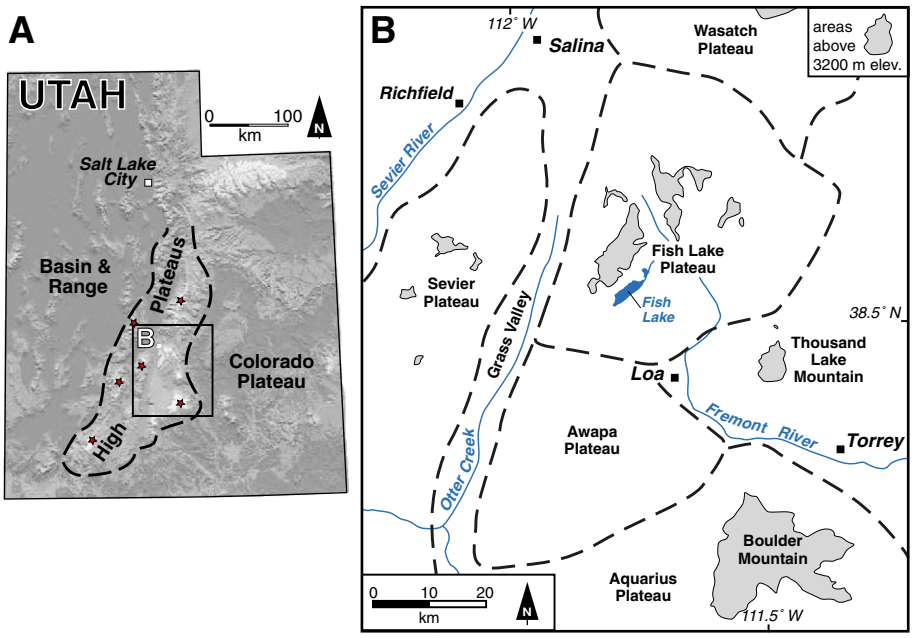

Figure 1. A. Location of the High Plateaus of Utah in the state of Utah. Other glaciated ranges in the High Plateaus are shown with red stars, see text for references. B. Location of the Fish Lake Plateau in the east central High Plateaus.

and Bevis, 2001) all have strong evidence for glaciation during the Pleistocene.

In this paper we use cosmogenic ^{3}He exposure age dating to determine the ages of glacial deposits from the Fish Lake Hightop Plateau in central Utah. We use reconstructions of former glacier extents to estimate local equilibrium-line altitudes (ELAs) during the LGM using the toe-to-headwall altitude ratio (THAR) and accumulation-area ratio (AAR) methods. Finally, we compare the modern climate at the reconstructed ELAs with modern glacial conditions to estimate changes in annual precipitation and ablation season temperature between the LGM and modern conditions at Fish Lake.

Geography and geology of the Fish Lake Plateau

The High Plateaus of Utah form a region of distinctive topography that separates the Colorado Plateau to the east from the Basin and Range to the west (Fig. 1). Extending for over 250 km southward from the Salt Lake City region to southern Utah, the High Plateaus include eight individual plateaus and ranges with a combined area greater than 15,000 km^2. The highest elevations reach 3600 m and at many locations the western edge of the High Plateaus forms a sharp topographic front with relief in excess of 1500 m (e.g. Wasatch Front, Cedar Breaks). The drainage divides between the Great Basin and Colorado River systems lie astride the High Plateaus.

The Fish Lake Plateau, located to the south-southeast of Salina, Utah and west of Capitol Reef National Park, occurs along the eastern edge of the High Plateaus and is bounded to the west by the south-trending Grass Valley, the Awapa Plateau to the south, Rabbit Valley to the east and transitions northward into southern Wasatch Plateau (Fig. 1). From west to east the Fish Lake Plateau includes the broad, high elevation, gently southeast-sloping Fish Lake Hightop (elev. 3546 m), the Fish Lake basin (elev. ~2700 m), and the southeast-sloping Mytoge Mountain (Fig. 2). Fish Lake (8.6×1.8 km), with an average depth of ~27 m is the largest natural mountain lake in Utah and drains to the northeast into Lake Creek (Fig. 2). The Fremont River heads at the confluence of Lake and Sevenmile Creeks now under Johnson Valley Reservoir (Fig. 2).

The Fish Lake Plateau is underlain by Cretaceous to Early Tertiary sedimentary units that are unconformably overlain by a thick sequence of Oligocene to Miocene volcanic rocks. The Cretaceous and Early Tertiary units crop out along the northern and northeastern part of the Fish Lake Plateau and include limestone, siltstone, sandstone, and conglomerate of the North Horn, Flagstaff, and Colton Formations (Williams and Hackman, 1971; Carbaugh and Bailey, 2009). The volcanic sequence is 250 to 700 m thick and comprises three distinct units that include from bottom to top: the porphyritic and pyroxene-bearing Johnson Valley Reservoir trachyandesite, the phenocryst-poor Lake Creek trachyte, and biotite-bearing Osiris trachyte (also regionally called the Osiris tuff: e.g. Williams and Hackman, 1971; Mattox, 1991; Bailey et al., 2007; Ball et al., 2009) . Most of the volcanic units are ash-flow deposits and likely derived from the Marysvale volcanic field in west-central Utah (Anderson and Rowley, 1975; Ball et al., 2009). Multiple ^{40}Ar/^{39}Ar ages on sanidines from the Osiris trachyte yield a mean age of 23.03 ± 0.08 Ma while a single whole rock ^{40}Ar/^{39}Ar age from the Lake Creek trachyte is 25.15 ± 0.14 Ma (Ball et al., 2009).

Glacial deposits on the Fish Lake Plateau

The glacial deposits on the Fish Lake Plateau were previously studied by Dutton (1880), Hardy and Muessig (1952), and Osborn and Bevis (2001). Hardy and Muessig (1952) suggested that there is evidence for two main glacial advances around the Plateau, which they termed Wisconsin I and II and estimate as being equivalent to Early and Late Wisconsin in age, respectively. They also describe evidence for significant erosive ice modification on several areas of the Fish Lake Hightop. Osborn and Bevis (2001) include the Fish Lake Plateau in their review of Great Basin glaciation and agreed with most of Hardy and Muessig's (1952) conclusions about the extent of the glacial deposits however they did not find significant erosive ice modification on the Hightop.

During the summers of 2005–2008 we conducted field, air photo, and satellite image surveys of the glacial deposits on the Fish Lake Plateau. The main focus of our investigation was the deposits around the Fish Lake Hightop Plateau, as these are the most obvious and extensive of the glacial deposits on the entire Plateau. Three glaciers extended from the Fish Lake Hightop Plateau proper: the Rock Canyon, Pelican Canyon, and Tasha Creek glaciers, while two independent cirque glacier complexes: the Jorgenson Creek and

https://doi.org/10.1016/j.yqres.2010.09.009 Published online by Cambridge University Press

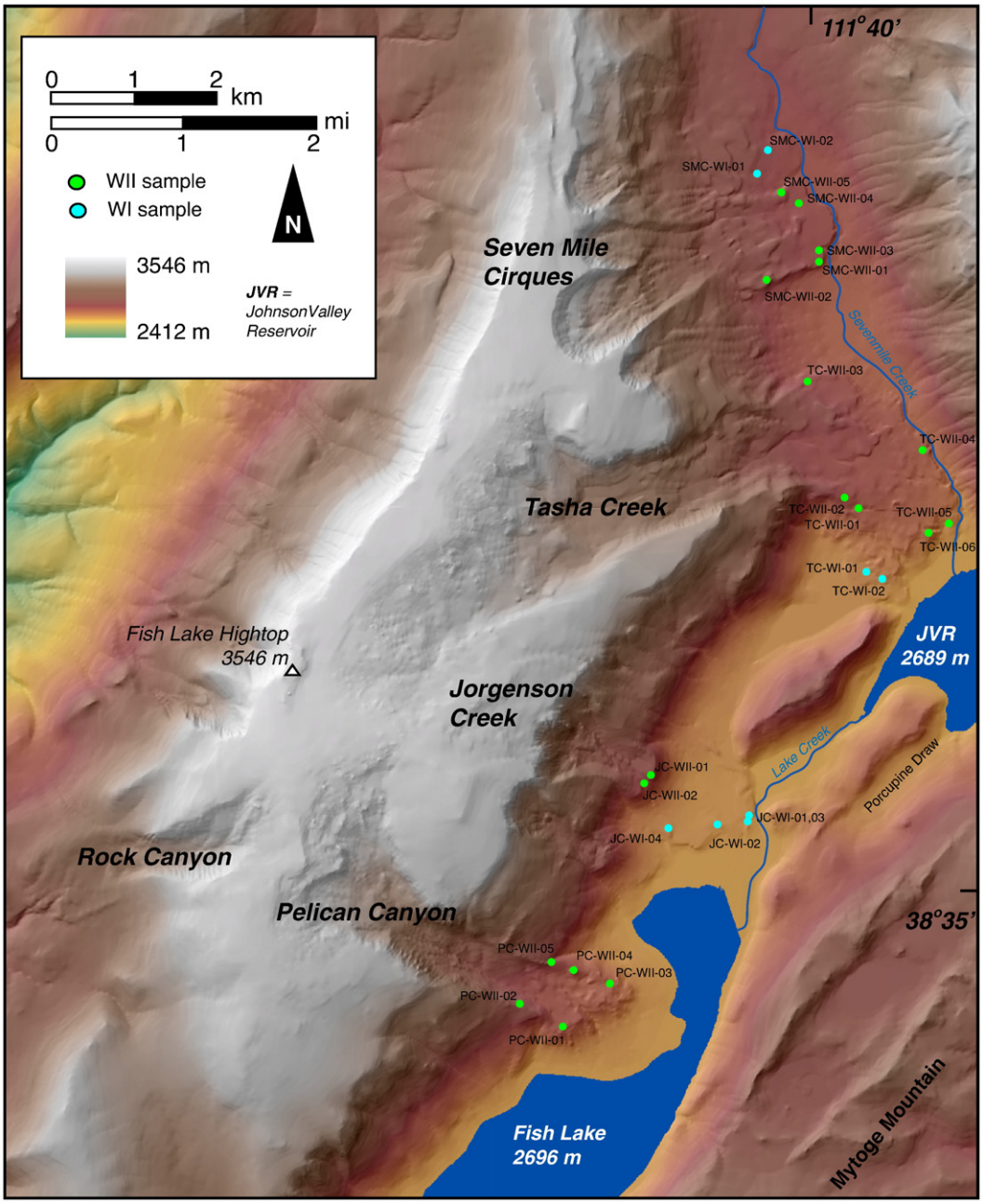

Figure 2. DEM and hillshade composite image of the Fish Lake Plateau Hightop and associated glacial deposits. Cosmogenic sample locations labeled.

Seven Mile, formed on the respective eastern and northeastern margins of the Hightop Plateau (Fig. 2).

Fish Lake Hightop

The Fish Lake Hightop may have hosted a small (~4 km^2) ice cap or permanent snow field with ice or snow spilling into three main glacial troughs. The Hightop does not have extensive evidence of erosive ice modification. The predominant volcanic unit on the Hightop is the Lake Creek trachyte, which commonly occurs as thin, platy sheets which are easily fractured and do not preserve grooving or striations. The strongest evidence of glacial erosion on the Hightop is the sculpting of the heads of the three main glacial outlets (Fig. 2). All three glacial outlets head on gently sloping sections off the Hightop and then become constricted, steep walled, glacial troughs that ultimately spill out onto the adjacent valley floors.

Rock Canyon

The glacier in Rock Canyon headed on the Hightop and descended to an elevation of ~2990 m (Fig. 2). The Rock Canyon glacier is the smallest of the glaciers from the Hightop, possibly due to increased ablation from its west-southwest aspect. A steep sided, hummocky, latero-terminal moraine loop defines the most recent advance of the Rock Creek glacier. Hardy and Muessig (1952) report an older glacial deposit to the north of the younger moraine. In the location of their older WI deposit we did find a slightly hummocky broad crested ridge; however it lacks convincing moranic topography and may be a

https://doi.org/10.1016/j.yqres.2010.09.009 Published online by Cambridge University Press

bedrock-cored ridge. Very few suitable boulders of the pyroxene-bearing Johnson Valley Reservoir trachyandesite unit occur on the Rock Canyon moraine which precluded using ^{3}He techniques to date this feature.

Pelican Canyon

The Pelican Canyon glacier headed on the Hightop and flowed off the Hightop through a ~200 m deep, ~1.5 km long trough cut through the main mass of volcanic rocks on the Plateau. A pair of steep-sided (20–25°) bouldery, lateral moraines define the margins of the youngest moraine. The toe of the youngest moraine is composed of several steep, yet short, ridges and hills with intervening closed depressions. The lowest elevation reached by the youngest Pelican Canyon glacier is ~2760 m. A few smaller recessional moraine sets are nested just upstream and interior to the terminal and lateral moraines. A gently sloping outwash fan is deposited radially from the terminal moraine body and is one of the most conspicuous surficial features in the Fish Lake basin, nearly isolating the main body of Fish Lake from Widgeon Bay (Fig. 2; Fig. S1). Hardy and Muessig (1952) recognized only one age of glacial deposits at Pelican Canyon, which they considered to be WII or late Wisconsin in age.

Bathymetric surveys of Fish Lake were conducted in the summers of 2005 and 2006 using a single-beam 200 kHz transducer linked to a Leica SR530 real-time kinematic global positioning system (RTK-GPS) with a base-station and rover setup for real-time corrections.

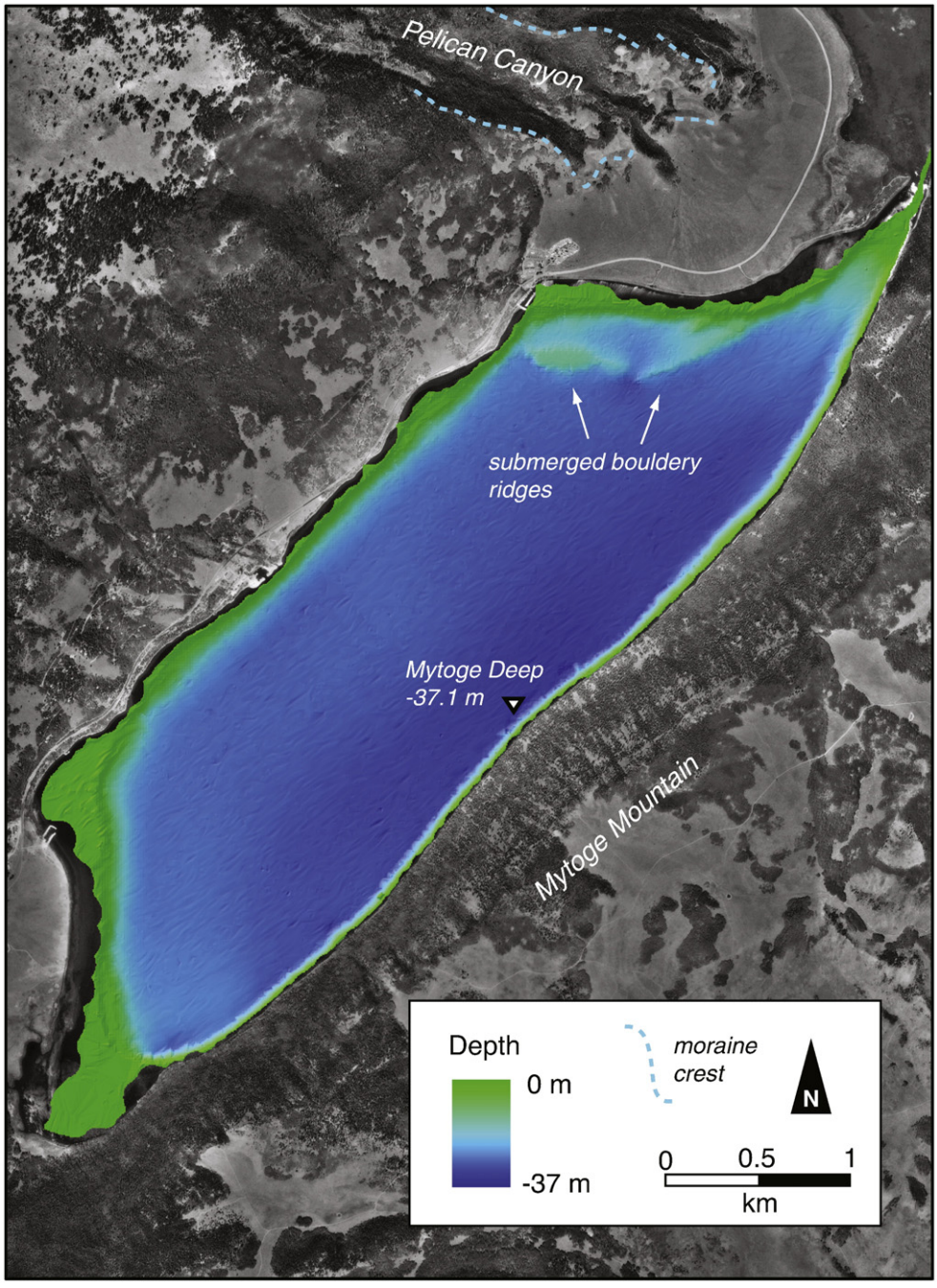

Figure 3. Bathymetric map of the main body of Fish Lake displayed on top of a digital orthophotograph. The northern segment of the lake was not surveyed due to its shallow depth and thick aquatic vegetation.

https://doi.org/10.1016/j.yqres.2010.09.009 Published online by Cambridge University Press

Horizontal positions were linked to depth soundings and merged in ArcPad. Accuracy for the fathometer is approximately 5–10 cm and for the RTK-GPS approximately 1–5 cm, giving a realistic accuracy of approximately 6–12 cm for the ~23,000 depth measurements across the lake. Data were gridded within ArcGIS and clipped to the shoreline. The resulting bathymetric map is shown in Figure 3. The image reveals a series of ridge-like features in ~20 m of water that are ~1 km to the south of the Pelican Canyon outwash fan. These slightly arcuate ridges are ~3 km long, project out ~10 m from the lake bottom, and are breached in a location coincident with the modern Pelican Canyon drainage. Side scan sonar (Marine Sonics 400 KHz, 150 m swath) indicates that the ridges are bouldery and easily distinguishable from the abundant lake bottom muds. We interpret this feature to be an older moraine ridge, likely correlative to Hardy and Muessig's (1952) WI unit and Bull Lake in age; however the subaqueous feature remains undated.

Jorgenson Creek Cirques

The two Jorgenson Creek glaciers formed in a series of steep cirques carved into the eastern edge of the Fish Lake Hightop plateau. The more northerly and larger of the Jorgenson Creek glaciers formed in a compound cirque and deposited two distinctly different moraines (Fig. 2; Fig. S1). The younger of these deposits is a steep-sided (25–30°), sharp-crested terminal moraine loop deposited by ice that descended to an elevation of ~2870 m. Approximately 400 to 800 m down valley of the younger moraine deposit is a second moraine loop. This feature has relatively gentle slopes (5–15°; except where incised), heavily weathered boulders, and a subdued surface topography. The older Jorgenson Creek deposits are much larger in areal extent than the younger deposits, and suggest ice was as low as ~2720 m during deposition of the older moraine (Fig. 2).

We found no field or air photo evidence of erosive ice modification on the Hightop Plateau above the Jorgenson Creek cirques. This contradicts Hardy and Muessig (1952), who mapped glacial features above the Jorgenson area on their glaciation map. We suspect that Hardy and Muessig (1952) misidentified a dipping contact of two different sub-units of the Lake Creek trachyte as an ice marginal ridge. The lack of evidence for erosive ice above, or ice spillover into, the Jorgenson area suggests that the Jorgenson Creek glaciers were constrained within their cirques and did not connect to an ice cap on the Hightop Plateau, at least during the last glaciation.

Tasha Creek

The Tasha Creek glacier was the largest glacier that headed on the Hightop Plateau. Ice flowed from a large accumulation area on the Hightop to the east-northeast, through a deep glacial trough (Fig. S2) cut into the northeastern margin of the Hightop Plateau and out onto Sevenmile valley. In the Sevenmile valley the glacier was deflected downstream towards the southeast. A complex, ~2 km long, assemblage of very hummocky, moderate-to-steep sided, moraines was deposited parallel to the course of Sevenmile Creek by the Tasha Creek glacier (Fig. 2).

Hardy and Muessig (1952) recognized two different ages of glacial deposits from Tasha Creek. We recognize only one; a young deposit likely correlative with the younger deposits elsewhere around the Hightop. Hardy and Muessig's (1952) WI deposit at Tasha Creek is likely the product of glacigenic mass wasting (formerly flow till) associated with the younger glaciation, as the feature originates from within the southern edge of the main moraine deposit. Several smaller recessional lateral moraines are inset upstream of the main body of the deposit. We estimate that ice flowed to an elevation of ~2720 m during the youngest glaciation at Tasha Creek.

Sevenmile Cirques

The Sevenmile cirques are the most northerly of the glacial features associated with the Hightop Plateau. Four steep-walled cirques hosted independent glaciers that spilled out onto the Sevenmile valley (Fig. 2; Fig. S2). The most northerly and southerly of the cirques supported glaciers that did not produce distinct terminal moraines. The two central cirques produced a merged body of glacial ice that flowed down to an elevation of ~2840 m. Deposits from the last advance from this glacier consist of a multi-lobed, steep sided (20–30°), latero-terminal moraine loop that encloses numerous ponds and depressions. A prominent set of recessional lateral moraine ridges are located $\leq$1.0 km upstream of the main terminal loop. We found no evidence of erosive ice modification or ice spill-over on the Hightop Plateau above the Sevenmile cirques, indicating that the accumulation areas of the individual glaciers were isolated within the cirques.

Hardy and Muessig (1952) mapped an older glacial deposit (WI) to the north of the toe of the younger set of deposits and moraines. In that location we found slightly hummocky boulder deposits with heavily weathered boulders and possible morainic topography. We agree with Hardy and Muessig (1952) and Osborn and Bevis (2001), that there may be an older glacial deposit in this location, however it is by no means definitive and it is difficult to accurately identify its margins.

Cosmogenic dating of glacial deposits

We measured cosmogenic ^{3}He concentrations in pyroxene separates from boulder samples taken from the crests of moraines from around the Fish Lake Hightop Plateau (Fig. 2). Our sampling strategy was to sample the highest (tallest) boulders that were sitting in stable positions on the crests of moraines (Table 1; Fig. S3). We only sampled boulders composed of the pyroxene-bearing Johnson Valley Reservoir trachyandesite, which is the most physically resistant rock unit exposed on the Plateau. We collected samples from boulders that had relatively flat, un-weathered top surfaces to reduce the possibility of boulder weathering affecting the exposure ages. Site data was collected with GPS units and verified with topographic maps (Table 1). The horizontal data are relative to the NAD 27 datum and boulder surface elevation uncertainties are likely less than $\pm$8 m.

Nucleogenic correction

The cosmogenic ^{3}He exposure age method has both advantages and disadvantages when compared to other routinely used cosmogenic exposure age techniques (e.g. ^{10}Be, ^{36}Cl, Gosse and Phillips, 2001). ^{3}He has the highest production rate of all the terrestrial cosmogenic isotopes and He isotopic concentrations can be measured relatively easily using conventional noble gas mass spectrometry. Major disadvantages of the method are that He is only quantitatively retained in a few mineral phases (e.g. Farley et al., 2001), and that there can be multiple sources of non-cosmogenic ^{3}He in many mineral phases.

In pyroxene, there are two main sources of non-cosmogenic ^{3}He: a mantle component ($^{3}He_m$) which, when present, is trapped in fluid inclusions (Kurz, 1986), and a nucleogenic component ($^{3}He_n$) produced from thermal neutron reactions on ^{6}Li (^{6}Li (n,α) ^{3}H ^{3}He) (Andrews and Kay, 1982). To correct for possible mantle-gas contamination in our samples we crushed multiple pyroxene samples on-line (under vacuum) and measured the He isotope concentrations in the released gasses. All of the crushed samples had negligible gas concentrations (close to the detection limit and line blanks) and unresolvable ^{3}He/^{4}He ratios, indicating that pyroxenes from volcanic rocks on the Fish Lake Plateau do not have a significant component of mantle-derived He.

We used completely shielded samples of the pyroxene bearing Johnson Valley Reservoir trachyandesite (Bailey et al., 2007) to correct

https://doi.org/10.1016/j.yqres.2010.09.009 Published online by Cambridge University Press

Table 1
Cosmogenic sampling data and production rates.

Location/sample	Latitude (N)	Longitude (W)	Elevation (m)	Boulder height/longest axis (m)	Topo shielding factor	Self-shielding factor	Total shielding factor	^{3}He production rate[a] (atoms g^{-1} yr^{-1})
Pelican Canyon								
PC-WII-01	38.5676	111.7013	2817	1.4/3.1	0.999	0.974	0.973	899
PC-WII-02	38.5708	111.7103	2941	1.1/2.8	0.998	0.957	0.955	952
PC-WII-03	38.5729	111.6943	2780	1.0/2.6	0.999	0.957	0.956	864
PC-WII-04	38.5740	111.6998	2845	0.8/2.3	0.999	0.957	0.956	899
PC-WII-05	38.5749	111.7034	2878	1.2/1.9	0.957	0.999	0.956	918
Jorgenson Creek								
JC-WII-01	38.5960	111.6893	2887	1.5/2.6	0.998	0.965	0.963	930
JC-WII-02	38.5959	111.6899	2886	1.7/2.7	0.998	0.974	0.972	937
JC-WI-01	38.5902	111.6757	2716	0.8/1.3	0.999	0.957	0.956	845
JC-WI-02	38.5905	111.6804	2728	0.9/1.5	0.998	0.942	0.940	837
JC-WI-03	38.5902	111.6755	2717	1.0/2.1	0.999	0.965	0.964	852
JC-WI-04	38.5896	111.6872	2737	0.9/2.2	0.999	0.965	0.964	863
Tasha Creek								
TC-WII-01	38.6238	111.6594	2807	1.5/3.2	0.999	0.957	0.956	880
TC-WII-02	38.6260	111.6628	2851	1.1/2.0	0.999	0.974	0.973	919
TC-WII-03	38.6392	111.6673	2865	1.1/2.6	0.999	0.965	0.964	919
TC-WII-04	38.6311	111.6505	2793	1.2/2.3	0.997	0.965	0.962	878
TC-WII-05	38.6231	111.6476	2726	1.2/1.7	0.998	0.974	0.972	850
TC-WII-06	38.6228	111.6493	2739	1.1/2.9	0.997	0.965	0.962	849
TC-WI-01	38.6173	111.6604	2739	1.2/2.3	0.998	0.940	0.938	827
TC-WI-02	38.6167	111.6571	2734	0.7/1.1	0.998	0.974	0.972	854
Seven Mile Cirques								
SMC-WII-01	38.6527	111.6662	2860	1.4/2.1	0.999	0.965	0.964	917
SMC-WII-02	38.6499	111.6735	2905	1.4/2.0	0.999	0.965	0.964	942
SMC-WII-03	38.6531	111.6661	2858	1.1/1.8	0.998	0.974	0.972	923
SMC-WII-04	38.6589	111.6683	2868	1.2/2.0	0.999	0.974	0.973	929
SMC-WII-05	38.6604	111.6703	2876	1.5/3.3	0.999	0.974	0.973	934
SMC-WI-01	38.6616	111.6739	2859	1.1/4.3	0.999	0.957	0.956	924
SMC-WI-02	38.6634	111.6732	2865	1.0/3.4	0.999	0.965	0.964	935

[a] Production rate determined using a high latitude, seal level production rate of 120 atoms g^{-1} yr^{-1} (Gohering et al., 2009), scaled using Lal (1991).

for nucleogenic ^{3}He in our cosmogenic samples. Marchetti and Cerling (2005) and Marchetti et al. (2005) describe the context of our suite of shielded samples. The shielded sample pyroxenes yielded ^{3}He concentrations ranging from 3.7×10^6 to 10.9×10^6 atoms g^{-1}, ^{4}He concentrations ranging from 18.25×10^{12} to 46.54×10^{12} atoms g^{-1}, and a very consistent ^{3}He/^{4}He ratio of 2.08×10^{-7} which was used to correct cosmogenic samples for nucleogenic ^{3}He (see below). Marchetti and Cerling (2005) and Marchetti et al. (2005) demonstrated that the ^{4}He in pyroxenes from shielded samples is solely radiogenic, while the ^{3}He was predominantly nucleogenic and in the cases of shielded samples from allochthonous deposits, partly from pre-exposure. Pyroxenes from rocks identical to the Johnson Valley trachyandesites on the nearby Boulder Mountain have a mean U concentration of 0.6 ppm, a mean Th concentration of 1.3 ppm, and Li concentrations that range from 13 to 38 ppm ($n=14$) with a mean of 22 ppm (Marchetti and Cerling, 2005).

Analytical

Pyroxene samples were concentrated through standard crushing and sieving. We used the 1–2 mm size fraction for our analyses and etched each pyroxene sample in 5% HF for 15 to 30 min, likely removing the outer few 10 s of μm of each pyroxene grain.

He isotope concentrations were measured using noble-gas mass spectrometry at the University of Utah Dissolved and Noble Gas Laboratory. Pyroxene separates were completely degassed in a Mo lined crucible at >1400°C. Reactive gasses were removed using SAES getters, while Ar and Ne were trapped and removed cryogenically. ^{3}He and ^{4}He concentrations were measured on a MAP-251 mass spectrometer using Farady cup (^{4}He) and electron multiplier (^{3}He) detectors. Measured counts of ^{3}He and ^{4}He were furnace-blank corrected and then standardized against multiple analyses of purified Yellowstone Park gas (MM) that has a known ^{3}He/^{4}He ratio of 16.5 R_A (where R_A is the ^{3}He/^{4}He ratio in air ~1.39×10^{-6}). Procedural furnace blanks in this system range from 0 to 2×10^5 atoms for ^{3}He and 1 to 5×10^9 atoms for ^{4}He.

Concentrations of cosmogenic ^{3}He (^{3}He$_c$) were determined from the total measured ^{3}He and ^{4}He concentrations (^{3}He$_{tot}$ and ^{4}He$_{tot}$) using the following relationship:

$$^3He_c = {}^3He_{tot} - \left[{}^4He_{tot} \times \left({}^3He/{}^4He\right)_s\right] \quad (1)$$

where the shielded (^{3}He/^{4}He)$_s$ ratio is 2.08×10^{-7} (Marchetti et al., 2005).The 1σ uncertainty associated with the shielded correction is ~14% and is propagated through the determinations of the ^{3}He$_c$ concentrations (Table 2).

Boulder exposure ages

The He isotope data and exposure ages are given in Table 2. Cosmogenic ^{3}He exposure ages were calculated using the ^{3}He$_c$ concentrations as determined above and a sea-level, high-latitude ^{3}He production rate of 120 atoms g^{-1} yr^{-1} (Goehring et al., 2009) scaled to each samples altitude, latitude, and total shielding (Table 1) using Lal (1991) and Gosse and Phillips (2001). The resulting exposure ages were not adjusted for boulder surface erosion. Exposure ages were adjusted for possible snow shielding using the method outlined in Gosse and Phillips (2001) and employing historic snow pack data from the nearby Black Flat-U.M. Creek Snotel Site (BFTU-1; www.cbrfc.noaa.gov/snow/station/sweplot/sweplot.cgi?

https://doi.org/10.1016/j.yqres.2010.09.009 Published online by Cambridge University Press

Table 2
Helium isotope data and exposure ages for cosmogenic samples.

Location/sample	$^4He_{tot}$ (10^{12} atoms g^{-1})	$^3He_{tot}$ (10^6 atoms g^{-1})	$^3He/^4He$ fusion	R/R_A fusion	^3He_c[a] (10^6 atoms g^{-1})	^3He_c %	Exposure age[b] (ka) $\pm 2\sigma$
Pelican Canyon							
PC-WII-01	16.22 ± 0.08	21.4 ± 0.5	1.32×10^{-6}	0.95	18.0 ± 0.9	84.3	20.5 ± 1.1
PC-WII-02	15.65 ± 0.10	25.2 ± 1.0	1.61×10^{-6}	1.16	21.9 ± 1.2	87.1	23.5 ± 1.3
PC-WII-03	25.79 ± 0.06	23.6 ± 1.1	9.14×10^{-7}	0.66	18.2 ± 1.4	77.3	21.5 ± 1.7
PC-WII-04	29.32 ± 2.05	21.7 ± 2.5	7.39×10^{-7}	0.53	15.6 ± 2.4	71.9	17.7 ± 2.8
PC-WII-05	22.68 ± 0.53	21.6 ± 0.2	9.51×10^{-7}	0.69	16.9 ± 1.1	78.2	18.8 ± 1.2
Jorgenson Creek							
JC-WII-01	23.76 ± 0.11	24.1 ± 0.8	1.02×10^{-6}	0.73	19.2 ± 1.3	79.5	21.1 ± 1.4
JC-WII-02	22.97 ± 0.05	24.0 ± 0.9	1.05×10^{-6}	0.76	19.2 ± 1.3	80.1	21.0 ± 1.4
JC-WI-01	24.86 ± 0.10	111.2 ± 1.7	4.47×10^{-6}	3.23	106.0 ± 2.2	95.4	128 ± 3
JC-WI-02	24.74 ± 0.14	69.4 ± 2.2	2.80×10^{-6}	2.03	64.2 ± 2.4	92.6	79 ± 3
JC-WI-03	26.89 ± 0.14	138.2 ± 3.8	5.14×10^{-6}	3.71	132.6 ± 4.0	96.0	159 ± 5
JC-WI-04	27.48 ± 0.11	134.2 ± 1.3	4.89×10^{-6}	3.53	128.5 ± 2.1	95.7	152 ± 3
Tasha Creek							
TC-WII-01	28.62 ± 0.11	18.8 ± 0.1	6.57×10^{-7}	0.48	12.9 ± 1.3	68.4	14.9 ± 1.5
TC-WII-02	25.57 ± 0.10	20.2 ± 1.2	7.92×10^{-7}	0.57	14.9 ± 1.4	73.8	16.6 ± 1.6
TC-WII-03	24.55 ± 0.13	28.1 ± 1.9	1.14×10^{-6}	0.83	22.9 ± 1.9	81.8	25.5 ± 2.2
TC-WII-04	27.94 ± 0.06	21.1 ± 0.8	7.53×10^{-7}	0.54	15.2 ± 1.3	72.4	17.8 ± 1.5
TC-WII-05	26.01 ± 0.06	193.0 ± 4.2	7.42×10^{-6}	5.36	187.6 ± 4.4	97.2	226 ± 6
TC-WII-06	23.47 ± 0.03	36.2 ± 1.5	1.54×10^{-6}	1.12	31.4 ± 1.7	86.5	38 ± 3
TC-WI-01	25.88 ± 0.11	23.1 ± 1.7	8.93×10^{-7}	0.65	17.7 ± 1.7	76.7	21.9 ± 2.2
TC-WI-02	23.30 ± 0.09	25.6 ± 1.3	1.10×10^{-6}	0.79	20.8 ± 1.6	81.1	24.8 ± 1.9
Seven Mile Cirques							
SMC-WII-01	20.96 ± 0.08	23.1 ± 0.6	1.10×10^{-6}	0.80	18.7 ± 1.1	81.1	20.9 ± 1.3
SMC-WII-02	20.38 ± 0.06	23.8 ± 0.7	1.17×10^{-6}	0.84	19.6 ± 1.2	82.2	21.2 ± 1.3
SMC-WII-03	21.99 ± 0.07	45.3 ± 1.0	2.06×10^{-6}	1.49	40.7 ± 1.5	89.9	45 ± 2
SMC-WII-04	24.66 ± 0.08	24.5 ± 1.1	9.92×10^{-7}	0.72	19.3 ± 1.4	79.1	21.3 ± 1.6
SMC-WII-05	33.64 ± 0.08	27.3 ± 0.8	8.12×10^{-7}	0.59	20.3 ± 1.6	74.4	22.3 ± 1.8
SMC-WI-01	26.03 ± 0.03	116.2 ± 2.5	4.46×10^{-6}	3.23	110.8 ± 2.8	95.3	123 ± 4
SMC-WI-02	20.97 ± 0.06	171.0 ± 2.9	8.16×10^{-6}	5.89	166.7 ± 3.2	97.5	182 ± 4

[a] ^3He_c determined using Eq. (1) and a $^3He/^4He$ shielded value of 2.08×10^{-7} (Marchetti et al., 2005).
[b] Exposure ages are determined using the ^3He_c concentration and corresponding production rate value from Table 1. The ages include a snow correction based on historic winter snowpack data from the nearby Black Flat / UM creek SNOTEL site using Gosse and Phillips, 2001 (see text).

BFTU1). This Snotel site is less than 15 km northeast of Fish Lake and is at a similar elevation (2867 m) to our sampled boulders, and so provides a good representation of the historic snow pack in the area. The snow correction added between 1.5% and 2.2% to the calculated exposure ages (Table 2).

Estimates of ELAs and climate during the last glacial maximum at Fish Lake, UT

The equilibrium line altitude (ELA) of alpine glaciers is a useful climatic indicator. If the ELA of paleoglaciers in formerly glaciated

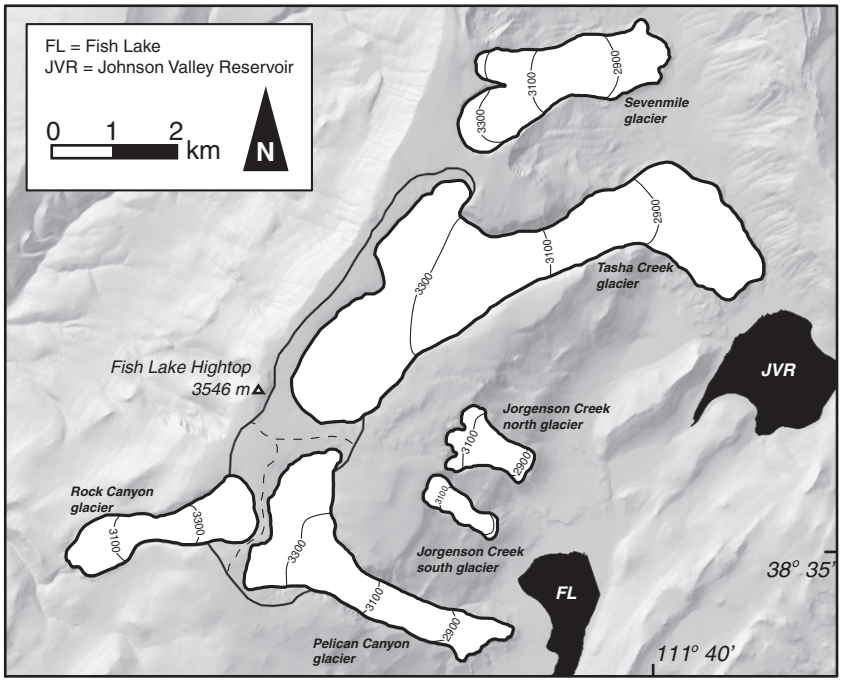

Figure 4. Reconstructions of LGM age glaciers on the Fish Lake Plateau. Contour lines are in meters and indicate reconstructed ice surface elevations.

https://doi.org/10.1016/j.yqres.2010.09.009 Published online by Cambridge University Press

Table 3
Paleoglacier ELA data.

Paleoglacier	Glacier area (km^2)	ELA from AAR method (m)	ELA from THAR method (m)
Cirque			
Reconstructed as individual glaciers (AAR = 0.6 ± 0.1; THAR = 0.4 ± 0.05)			
Jorgenson Creek South	0.5	3020 ± 30	3035 ± 30
Jorgenson Creek North	0.9	2980 ± 20	3020 ± 20
Seven Mile	3.5	2950 +70/−40	3060 ± 30
Hightop			
Reconstructed as individual glaciers (AAR = 0.6 ± 0.1; THAR = 0.4 ± 0.05)			
Rock Canyon	2.1	3130 +100/−30	3165 ± 25
Pelican Canyon	4.2	3190 +50/−110	3030 ± 40
Tasha Creek	11.3	3130 +90/−140	3020 ± 40
Reconstructed as part of an ice cap (AAR = 0.7 ± 0.1)			
Rock Canyon	3.1	3190 +160/−90	n.a.
Pelican Canyon	5.1	3180 +80/−170	n.a.
Tasha Creek	13.5	3080 +150/−90	n.a.

areas can be reliably determined, then estimates of the climate changes needed to glaciate the area can be inferred (Leonard, 1989; Brugger and Goldstein, 1999). There are several techniques available to estimate the ELAs of formerly glaciated areas. Most of these methods involve determining the former glacier extent and measuring variables related to the glaciers area or elevation distribution and comparing those to identical variables on modern glaciers at equilibrium. All of these methods have significant uncertainties and can be confounded when glaciers have excessive supraglacial debris (Clark et al, 1994), or are significantly "piedmont" or "ice cap" like in their ice distribution (Leonard, 1984; Rea et al., 1998). Despite these potential problems, glacier reconstructions utilizing ELAs have been one of the most useful techniques in estimating the climates of past glaciations and the LGM and subsequent deglaciation in particular (e.g. Porter, 1975; Munroe and Mickelson, 2002; Denton et al., 2005).

In this report we used the accumulation-area ratio (AAR) and toe-to-headwall altitude ratio (THAR) methods to estimate the ELAs of Pinedale-age glaciers around the Fish Lake Hightop Plateau. More information about the AAR and THAR techniques are given in Meierding (1982), Torsnes et al. (1993), and Benn and Evans (1998). Paleoglaciers were reconstructed in ArcGIS using air photo, DEM, and satellite imagery. Glacier margins were mapped using lateral and terminal moraines, trim lines in glacially carved canyons, and erosional features in accumulation areas. Ice thicknesses were estimated along the course of reconstructed glacier beds with equations relating ice thickness, slope, and basal shear stress using modified versions of Locke (1995) (Fig. 4). We made minor adjustment to the thickness of each

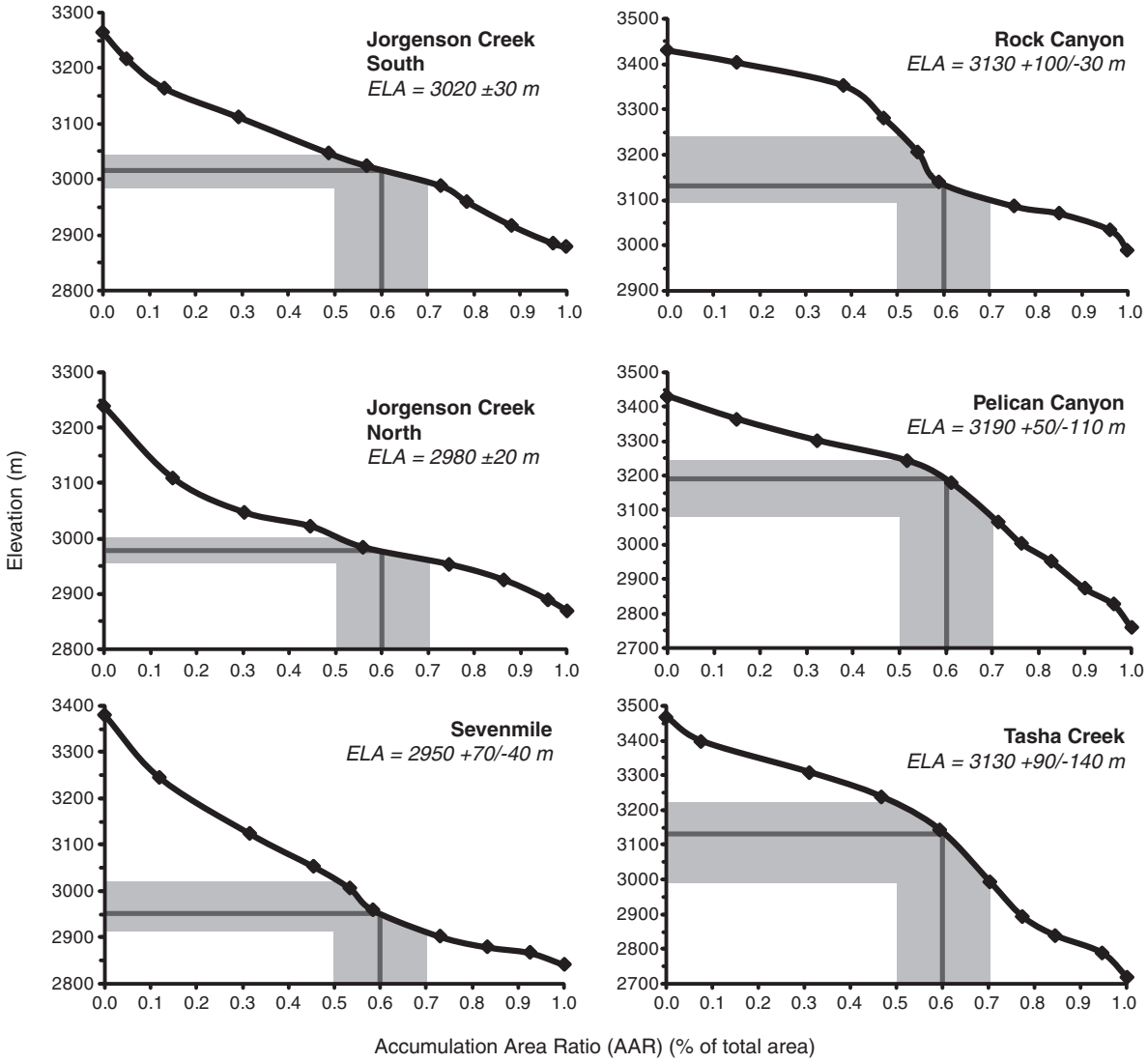

Figure 5. Elevation vs. total glacier area used to reconstruct glaciers using the AAR method. Hightop glaciers are modeled as individual glaciers. The gray boxes indicate the uncertainty (±0.1) associated with the AAR method and resultant uncertainty in the reconstructed ELAs (see text).

https://doi.org/10.1016/j.yqres.2010.09.009 Published online by Cambridge University Press

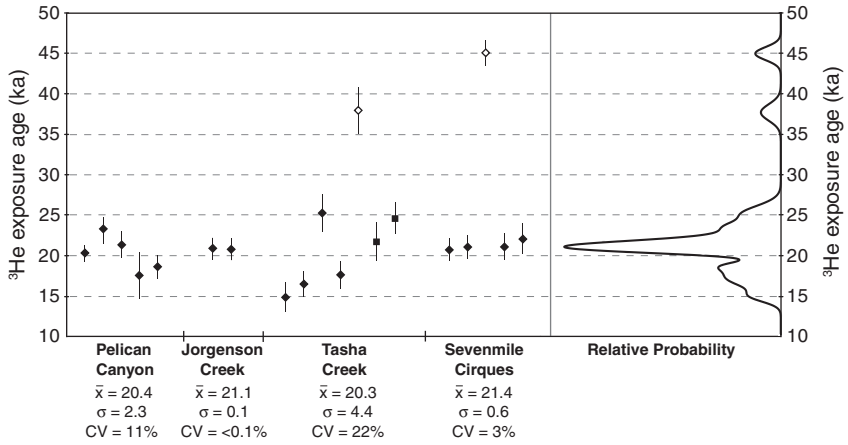

Figure 6. Exposure age data for the younger (WII) moraines sampled in this study. Squares indicate the boulders from the glacigenic mass movement feature associated with the Tasha Creek moraine. Open symbols indicate outliers. Sample TC-WII-05 (226 ± 6 ka) is not shown on the figure. The relative probability includes all the data shown on the figure. The outliers and relative probability were determined using ISOPlot (Ludwig, 1996).

paleoglacier so that the basal shear stress along the bed of each glacier was between 50 and 150 kPa (Paterson, 1994). We used a value of 0.4 ± 0.05 for the toe-to-headwall altitude ratio and 0.6 ± 0.1 and 0.7 ± 0.1 for the accumulation area ratio in the reconstructions of ELAs. The two different values and high uncertainties associated with the AAR ratios are due to the wide range of glacier types at Fish Lake (Table 3). The glaciers at Fish Lake range from simple cirque glaciers with well-constrained margins and relatively simple shapes (Sevenmile and Jorgenson Creek) to more complicated transection or outlet-type glaciers from the Fish Lake Hightop that may have been at least partially sourced from a small ice cap (Rock and Pelican Canyons, Tasha Creek). Typically, ice cap fed or transection glaciers would have a higher AAR, closer to 0.7 or 0.8 (Pierce, 1979; Rea et al., 1998). However, some of the glaciers from the Fish Lake Hightop are also piedmont like in their lower reaches as they spill out from constricted glacial canyons onto flat valley floors. Piedmont-type glaciers are thought to have a lower AAR values, on the order of ~0.5 (Leonard, 1984). So to capture the full range of possible glacier AAR relationships we reconstructed all the cirque glaciers using an AAR of 0.6 ± 0.1, and the Hightop glaciers in two different ways. The first Hightop glacier reconstruction assumed that the glaciers were not significantly fed from an ice cap and so we delineated the uppermost accumulation zone based on the margin of definitive ice erosion. In this scenario, the glaciers were reconstructed as separate glaciers. The ELAs of these glaciers were determined using an AAR of 0.6 ± 0.1 (Fig. 5). In the other scenario we reconstructed the Hightop glaciers assuming that their accumulation areas were connected and fed by a small ice cap or ice field, and we used an AAR of 0.7 ± 0.1 to estimate the ELAs of the merged glaciers.

We used the methods of Leonard (1989, 2007) to estimate LGM climatic conditions from our reconstructed paleoglacier ELAs. In this method the modern climatic conditions at the reconstructed paleoglacier ELAs are compared to modern climatic conditions at modern glacier ELAs. The difference between the values is an estimate of the temperature or precipitation changes needed to sustain the paleoglaciers at equilibrium during the LGM, and hence is an estimate of the range of possible temperature and precipitation changes between the LGM and today. We used the annual precipitation (cm H_2O) versus the summer (JJA) temperature (°C) data set in Ohmura et al. (1992) as the basis for the modern glacier ELA relationships.

To determine the modern climatic conditions at our range of reconstructed ELAs we used a linear regression of mean summer (JJA) temperature data versus elevation for multiple stations across central Utah (mean summer temperature (°C) = −0.0063 × elevation (m) + 31.293; $n = 43$; $r^2 = 0.946$; $p \ll 0.05$) (data from WRCC, 2006). The temperature data span elevations exceeding the range of reconstructed ELAs so no extrapolation was needed. The modern precipitation data were determined from annual precipitation values in the PRISM dataset (http://gisdev.nacse.org/prism/nn/index.phtml) (PRISM Climate Group, 2010). The 1971–2000 climate normals (30-arcsecond (~800 m) grid cell time series analysis from the PRISM data explorer) yield annual precipitation values of 85.4 to 95.5 cm (H_2O equivalent) for the range of reconstructed ELAs at Fish Lake. We use the mean of those two values (90.5 cm) as the estimate of modern annual precipitation for the range of reconstructed ELAs.

Discussion

Ages of glacial deposits

The exposure ages of moraine boulders from Fish Lake are given in Table 2 and Figure 6. The data include three locations where we determined ages of glacial deposits originally interpreted as Wisconsin I in age (early Wisconsinan, likely Bull Lake equivalent) by Hardy and Muessig (1952). From the south to the north these include the JC-WI, TC-WI, and SMC-WI samples (Table 1; Fig. 2).

The JC-WI samples range from 79 ± 3 to 159 ± 5 ka with a mean (± standard deviation) of 129 (± 39) ka. Exposure age populations from older, eroded moraines are notoriously difficult to interpret due to prolonged boulder erosion and potential boulder exhumation from deposit erosion (Hallet and Putkonen, 1994; Phillips et al., 1997; Putkonen and Swanson, 2003). Given those two factors we suspect

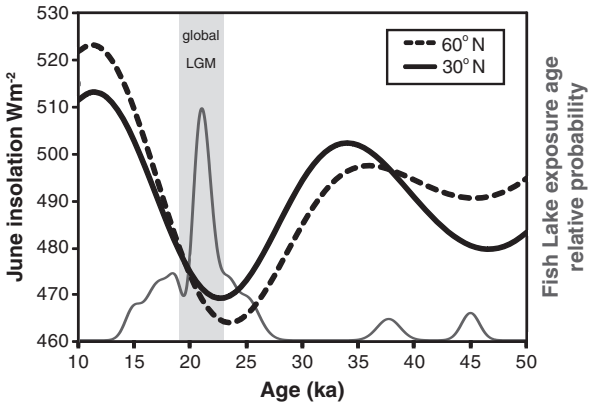

Figure 7. Summer insolation values for 30°N and 60°N between 10 and 50 ka (Berger and Loutre, 1991). The Fish Lake exposure age relative probability curve is shown in gray.

https://doi.org/10.1016/j.yqres.2010.09.009 Published online by Cambridge University Press

that the mean age of the JC-W1 deposit is an underestimate of the true age of the feature. Other cosmogenic studies of older, likely Bull Lake age moraines in the western U.S. have reported similar exposure age populations and concluded that the oldest exposure ages are likely the best indicator of the true age of moraine abandonment (Easterbrook et al., 2003; Licciardi and Pierce, 2008). If that is the case, then the JC-WI deposit was deposited ca. 152–159 ka and is likely Bull Lake (~MIS 6) in age (Easterbrook et al., 2003, Sharp et al., 2003).

The two ages from the TC-WI deposit indicate that the feature is not Bull Lake in age but rather LGM in age (Table 2). We previously discussed this feature (see above), and indicated that it is likely a glacigenic mass movement deposit associated with the younger set of glacial deposits at Tasha Creek. The two variable ages of the SMC-WI deposit only allow us to suggest that the feature is certainly older than the LGM and may be a Bull Lake age moraine, or may be older.

Exposure age samples from the younger WII moraines were originally thought to be late Wisconsin in age (LGM or Pinedale-age; Hardy and Muessig, 1952; Osborn and Bevis, 2001). The exposure ages confirm that age assignment, and analysis of the relative probability distribution of all the WII exposure ages suggests that the local LGM at Fish Lake occurred at ~21.1 ± 1.2 ka (sharp peak in relative probability curve in Fig. 6). This timing is coincident with the global LGM (21 ± 2 ka) and indicates that the Fish Lake glaciers reached their maximum extent at the end of an insolation minimum (Fig. 7) (Berger and Loutre, 1991). The statistical data associated with the exposure age populations (Fig. 6) indicate that moraines deposited from Hightop glaciers have greater variability than cirque constrained glaciers, when obvious outliers are excluded (TC-WII-05, TC-WII-06, SMC-WII-03).

The exposure ages from the Tasha Creek moraine boulders are highly variable. Even with two outliers removed, the ages have the highest variability of all the WII ages around the basin (Table 2). This is partly due to samples TC-WII-01 and TC-WII-02 which were collected from a higher elevation section of the right lateral moraine (Fig. 2) that may have been re-occupied by ice during a recessional event. The TC-WII suite of samples contributes to the 15–18 ka sub-peak in the relative probability curve (Fig. 6) and suggests that there may have been a re-advance or standstill of glacial ice at that time.

ELAs and LGM climate estimates at Fish Lake

ELA estimates are given in Table 3 and the LGM-to-modern climate changes are given in Table 4. The reconstructed LGM-age glacier ELAs range from 2950 to 3190 m. Glaciers descending from the Hightop have the highest ELAs while the cirque constrained glaciers have lower ELAs. This may be due to greater insolation on the exposed Hightop and late afternoon shading and favorable lee side snow accumulation of the southeasterly and northeasterly facing cirque glaciers. The ELAs determined using the THAR and AAR methods are similar for the cirque glaciers but differ for the Hightop glaciers. The two different Hightop glacier reconstructions (individual vs. ice cap) using the AAR method yielded very similar results, between 3100 and 3200 m.

Table 4
Possible precipitation and summer temperature depression conditions for the Fish Lake Plateau during the LGM.

Modern glacier data set	Annual precipitation (compared to modern)	Summer temperature depression (modern to LGM: °C)
World (maximum estimate)	0.5×	−12.1
	1.0×	−10.6
	1.5×	−9.2
	2.0×	−7.9
	3.0×	−5.9
Rocky Mountain (minimum estimate)	0.5×	−9.6
	1.0×	−8.1
	1.5×	−6.7
	2.0×	−5.5
	3.0×	−3.4

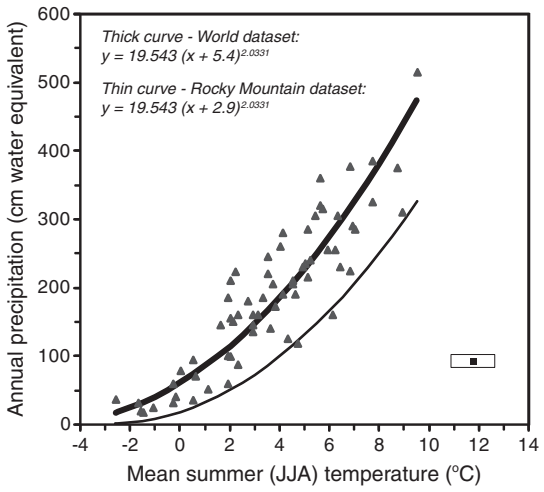

Figure 8. Annual precipitation vs. mean summer temperature for the modern glaciers in the Ohmura et al (1992) data set. The thick curve indicates the best fit for the entire (world) data set. The thin curve indicates the best fit for the Rocky Mountain part of the data set. Equations for lines are from Leonard (2007). The black square surrounded by the rectangle indicates the range of modern precipitation and mean summer temperatures determined for the reconstructed LGM ELAs at Fish Lake. To estimate the change in summer temperature between the LGM and today we subtracted the mean modern summer temperature at the reconstructed ELAs (black square) from the thick curve (maximum estimate) and the thin curve (minimum estimate) for varying precipitation amounts relative to the modern value of 90.5 cm (0.5×, 1×, 1.5×, 2×, 3×) (Table 4).

The climatic changes from modern conditions that are needed to sustain the LGM age paleoglaciers can be estimated from Fig. 8. The possible LGM-to-modern climatic changes are strongly dependant on which part of the Ohmura et al. (1992) data set (curve in Fig. 8) is used for comparison. Leonard (2007), following Locke (1989) and Braithwaite et al. (2006), makes the argument that glacier reconstructions in the western U.S. should use the Rocky Mountain data in the Ohmura et al. (1992) data set (thin line in Fig. 8) as the western U.S. is more likely associated with the higher temperature, lower precipitation part of the data set. This effectively provides a minimum estimate of the summer temperature depressions and led Leonard (2007) to suggest that using the Rocky Mountain data set may underestimate LGM to modern summer temperature depressions. We use the Rocky Mountain data set reconstruction (thin line in Fig. 8) in Table 4 as a minimum estimate of LGM to modern summer temperature depressions for various precipitation scenarios and the world data set (thick line in Fig. 8) as a maximum estimate of summer temperature depressions. Given those boundaries and assuming modern precipitation amounts, the Fish Lake Plateau likely had summer temperature depressions of −10.7 to −8.2°C during the LGM (Table 4).

Several studies around the central Rocky Mountains have documented LGM summer temperature depressions from paleoglacier ELA based reconstructions (Munroe and Mickelson, 2002 Brugger, 2006; Laabs et al., 2006; Leonard, 2007; Brugger, 2010). In these studies, summer temperature depressions for the LGM range from −6.5 to −9.5°C, assuming modern precipitation amounts. To bring the Fish Lake summer temperature depressions into that range would require increasing precipitation by 1.5× modern (Table 4). Therefore we suggest that the Fish Lake region may have had a slight increase in precipitation during the LGM compared to modern values.

Implications for regional paleoclimate

Our Fish Lake exposure age data adds to a growing body of research on the timing of LGM alpine deglaciation in the interior western US. The

https://doi.org/10.1016/j.yqres.2010.09.009 Published online by Cambridge University Press

Fish Lake data indicates local LGM moraine stabilization at ~21 ka and possible glacial re-advance or standstill at ~15–18 ka only a minimal distance upstream of the LGM position. This is similar to a number of glacial records across a wide range of latitudes in the interior western US. The following locations all have well-documented records of Pinedale-age terminal moraine stabilization during the LGM (21 ± 2 ka) and exposure ages on recessional moraines either at, or only slightly upstream of the LGM positions, between 15 and 18 ka: the Wallowa Mountains, OR (Licciardi et al., 2004); the Wind River Range, WY (Gosse et al., 1995; Easterbrook et al., 2003); the eastern Uinta Mountains, UT (Laabs et al., 2009); the eastern and western drainages of the Sawatch Range, CO (Brugger, 2007; Briner, 2009); and the Rio Grande drainage of the San Juan Mountains, CO (Benson et al., 2005). Glacial records from Boulder Mountain, UT (Marchetti et al., 2005; 2007); the Middle Boulder Creek Valley of the Colorado Front Range (Ward et al., 2009); and the Animas drainage of the San Juan Mountains, CO (Guido et al., 2007) all have roughly same timing of glaciations (terminal moraine at ~21 ± 2 ka; followed by retreat and re-advance or standstill until 15–18 ka) but these locations had more glacial retreat during the LGM to 15–18 ka time interval. Data from the Yellowstone ice cap and Teton Mountains (Licciardi and Pierce, 2008); the central Wasatch Mountains (Lips et al., 2005; Laabs et al., 2007); and the western Uinta Mountains (Laabs et al., 2009) document locations that had terminal moraine abandonment *after* the LGM and during 15–18 ka. For the Yellowstone and Teton records this may have been due to the complex dynamics of such a large ice cap and movement of the ice divide through time or moisture starvation during the LGM caused by anti-cyclonic flow off of the southern Laurentide ice sheet blocking moisture laden westerly storms (Licciardi and Pierce, 2008). The Wasatch and western Uinta locations are immediately downwind of pluvial Lake Bonneville and likely had prolonged glaciations due to lake-enhanced snowfall lowering ELAs until Lake Bonneville fell below the Provo level at 14–15 ka (Munroe and Mickelson, 2002; Godsey et al., 2005; Munroe et al., 2006; Laabs et al., 2009). The Fish Lake Plateau was likely too far from Lake Bonneville at all lake levels to supply significant lake-enhanced snowfall to the area. Several other ranges in the High Plateaus that were closer to Lake Bonneville may have had lake-enhanced precipitation affect paleoglacier ELAs (Mulvey, 1985).

Taken together, the glacial records for the interior western US indicate a broad synchrony in the timing of final LGM deglaciation (Schaefer et al., 2006). Most ranges began initial deglaciation during the LGM and then had a standstill or re-advance during the interval between 15 and 18 ka. Some ranges either did not have glaciers at their terminal positions during the LGM, or had post-LGM advances (15–18 ka) that overran the LGM moraines. It is clear that most of the interior western US glacier records document glaciers near, or at, their terminal moraine positions *after* the LGM and between 15 and 18 ka. This indicates sustained glaciation during a time period (15–20 ka) of increasing (5–7 Wm^{-2} per ka) ablation season insolation (Fig. 7). Hypotheses to explain how glaciers were sustained near their terminal moraine positions during a period of increasing insolation typically invoke additional moisture sources (e.g. Licciardi et al., 2004; Munroe et al., 2006; Thackray, 2008). For the Wasatch and western Uinta records this moisture was clearly from lake-enhanced precipitation off of Lake Bonneville (e.g. Laabs et al., 2009). For other locations the excess moisture is sometimes hypothesized to have come from low-pressure storms tracking along the polar branch of the Northern Hemisphere jet stream (e.g. Thackray, 2008), which was deflected significantly south of its present mean position due to the Laurentide ice sheet (Bartlein et al., 1998). Southward deflection of the polar jet stream during the LGM and possibly until ~14–15 ka is supported by modeling studies (Bartlein et al., 1998; Kutzbach et al., 1998) and several data sets from around the southwestern US (Jewell, 2007; Asmerom et al., 2010; Wagner et al., 2010). However, the jet stream hypothesis is somewhat contradicted by the fact that interior western US mountain ranges spanning a total of ~8° of latitude, have the same timing of final LGM deglaciation. It seems unlikely that jet-stream-driven storminess alone could supply the needed moisture across such a wide range of latitudes over several millennia. Further research into the climatic conditions across the interior western US during the 15–21 ka time interval and modeling studies of the dynamics of paleoglacier ELA responses to increasing insolation and seasonal precipitation changes (e.g. Fujita, 2008; Rupper et al., 2009) may provide a clearer resolution to this problem.

Conclusions

The Fish Lake Plateau hosted outlet and cirque glaciers at least twice during the Pleistocene. Exposure ages of boulders on an older, degraded moraine range from 79 to 159 ka and suggest deposition coincident with the type Bull Lake glaciation (MIS 6). Multiple boulders on younger moraines indicate a local LGM of ~21.1 ka while two ages from the Tasha Creek moraine may suggest a deglacial pause at 15–18 ka. ELAs of Pinedale-age glaciers range from 2950 to 3190 m and appear to be weakly controlled by aspect. Paleoglacier ELA reconstructions are relatively insensitive to the reconstruction method (AAR vs. THAR) and whether Hightop outlet glaciers were considered as part of an ice cap or as independent glaciers. LGM climate estimates from the paleoglacier ELAs suggest that with no change in precipitation, summer temperatures at Fish Lake were −10.7 to −8.2°C colder than modern. When compared to a regional data set of summer temperature depressions our data suggest that LGM precipitation at Fish Lake was either similar to modern or slightly increased (~1.5× modern).

Supplementary materials related to this article can be found online at doi:10.1016/j.yqres.2010.09.009.

Acknowledgments

We thank Kip Solomon and Alan Rigby at the Dissolved and Noble Gas Laboratory of the University of Utah for help with noble gas mass spectrometry. Scott Hynek, Will Weaver III, Danelle Stoll, Sarah Able, Andrew Heger, and Claire Pitcher assisted with cosmogenic sampling, field mapping, and mineral separation. The Loa, Utah office of the U.S. Forest Service provided logistical support. We thank Eric Leonard and Fred Phillips for reviews that improved this paper. This research was partly supported by the NSF (EAR-0453513 to Bailey and Harris), the University of Utah, Western State College of Colorado, the College of William and Mary, and the U.S. Geological Survey's EDMAP program.

References

Anderson, J.J., Rowley, P.D., 1975. Cenozoic stratigraphy of southwestern High Plateaus of Utah. Cenozoic geology of southwestern High Plateaus of Utah: In: Anderson, J.J., Rowley, P.D., Fleck, R.J., Nairn, A.E.M. (Eds.), Geological Society of America Special Paper, 160, pp. 1–51.

Andrews, J.N., Kay, R.L.F., 1982. Natural production of tritium in permeable rocks. Nature 298, 361–363.

Asmerom, Y., Polyak, V., Burns, S., 2010. Variable winter moisture in the southwestern United States linked to rapid glacial climate shifts. Nature Geoscience 3, 114–117.

Bailey, C.M., Harris, M.S., Marchetti, D.W., 2007. Geologic overview of the Fish Lake Plateau, Utah. Central Utah – diverse geology of a dynamic landscape: In: Willis, G.C., Hylland, M.D., Clark, D.L., Chidsey Jr., T.C. (Eds.), Utah Geological Association Publication, 36, pp. 47–55.

Ball, J.L., Bailey, C.M., Kunk, M.J., 2009. Volcanism on the Fish Lake Plateau, central Utah. Geological Society of America Abstracts with Programs 41 (6), 17.

Bartlein, P.J., Anderson, K.H., Anderson, P.M., Edwards, M.E., Mock, C.J., Thompson, R.S., Webb, R.S., Webb, T.I., Whitlock, C., 1998. Paleoclimate simulations for North America over the past 21,000 years: features of the simulated climate and comparisons with paleoenvironmental data. Quaternary Science Reviews 17, 549–585.

Benn, D.I., Evans, D.J.A., 1998. Glaciers and Glaciation. Arnold Publishers, London. 734 pp.

Benson, L., Madole, R., Landis, G., Gosse, J., 2005. New data for Late Pleistocene Pinedale alpine glaciations from southwestern Colorado. Quaternary Science Reviews 24, 49–65.

Berger, A., Loutre, M.F., 1991. Insolation values for the climate of the last 10 million years. Quaternary Sciences Review 10, 297–317.

Braithwaite, R.J., Raper, S.C.B., Chutko, K., 2006. Accumulation at the equilibrium-line altitude of glaciers inferred from a degree-day model and tested against field observations. Annals of Glaciology 43, 329–334.
Briner, J.P., 2009. Moraine pebbles and boulders yield indistinguishable ^{10}Be ages: a case study from Colorado, USA. Quaternary Geochronology 4, 299–305.
Brugger, K.A., 2006. Late Pleistocene climate inferred from the reconstruction of the Taylor River glacier complex, southern Sawatch Range, Colorado. Geomorphology 75, 318–329.
Brugger, K.A., 2007. Cosmogenic ^{10}Be and ^{36}Cl ages from Late Pleistocene terminal moraine complexes in the Taylor River drainage basin, central Colorado, USA. Quaternary Science Reviews 26, 494–499.
Brugger, K.A., 2010. Climate in the southern Sawatch Range and Elk Mountains, Colorado, U.S.A., during the Last Glacial Maximum: Inferences using a simple degree-day model. Arctic, Antarctic, and Alpine Research 42, 164–178.
Brugger, K.A., Goldstein, B.S., 1999. Paleoglacier reconstruction and late-Pleistocene equilibrium-line altitudes, southern Sawatch Range, Colorado. Glacial Processes Past and Present: In: Mickelson, D.M., Attig, J.W. (Eds.), Geological Society of America, Special Paper, 337, pp. 103–112.
Carbaugh, J.E., Bailey, C.M., 2009. Sedimentary geology of the northern Fish Lake Plateau, central Utah. Geological Society of America Abstracts with Programs 41 (6), 37.
Clark, D.H., Clark, M.M., Gillespie, A.R., 1994. Debris-covered glaciers in the Sierra Nevada, California, and their implications for snowline reconstructions. Quaternary Research 41, 139–153.
Clark, P.U., Dyke, A.S., Shakun, J.D., Carlson, A.E., Clark, J., Wohlfarth, B., Mitrovica, J.X., Hostetler, S.W., McCabe, A.M., 2009. The Last Glacial Maximum. Science 325, 710–714.
Currey, D.R., Mulvey, W.E., Lindsay, L.M.W., 1986. Markagunt Plateau, Southern margin of late Wisconsinan glaciations in the Great Basin. Programs and Abstracts—American Quaternary Association 35a (9), 126.
Denton, G.H., Alley, R.B., Comer, G., Broecker, W.S., 2005. The role of seasonality in abrupt climate change. Quaternary Science Reviews 24, 1159–1182.
Dutton, C.E., 1880. Report on the geology of the High Plateaus of Utah. U.S. Geographical and Geological Survey of the Rocky Mountains Region (Powell), xxxii, Washington DC, p. 307.
Easterbrook, D.J., Pierce, K., Gosse, J., Gillespie, A., Evenson, E., Hamblin, K., 2003. Quaternary geology of the western United States. In: Easterbrook, D.J. (Ed.), Quaternary geology of the United States, INQUA 2003 Field Guide Volume. Desert Research Institute, Reno, NV, pp. 19–79.
Farley, K.A., Cerling, T.E., Fitzgerald, P.G., 2001. Cosmogenic ^{3}He in igneous and fossil tooth enamel fluorapatite. Earth and Planet Science Letters 185, 7–14.
Flint, R.F., Denny, C.S., 1958. Quaternary Geology of Boulder Mountain Aquarius Plateau, Utah. Geological Survey Bulletin 1061-D, 103–164.
Fujita, K., 2008. Effect of precipitation seasonality on climatic sensitivity of glacier mass balance. Earth and Planetary Science Letters 276, 14–19.
Godsey, H.S., Currey, D.R., Chan, M.A., 2005. New evidence for an extended occupation of the Provo shoreline and implications for regional climate change, Pleistocene Lake Bonneville, Utah, USA. Quaternary Research 63, 212–223.
Goehring, B.M., Kurz, M., Balco, G., Schaefer, J.M., Licciardi, J., Lifton, N., 2009. A reevaluation of in-situ cosmogenic ^{3}He production rates. Geological Society of America Abstracts with Programs 41 (7), 649.
Gosse, J.C., Phillips, F.M., 2001. Terrestrial in situ cosmogenic nuclides: theory and application. Quaternary Science Reviews 20, 1475–1560.
Gosse, J.C., Klein, J., Evenson, E.B., Lawn, B., Middleton, R., 1995. Beryllium-10 dating of the duration and retreat of the last Pinedale glacial sequence. Science 268, 1329–1333.
Guido, Z.S., Ward, D.J., Anderson, R.S., 2007. Pacing the post-Last Glacial Maximum demise of the Animas Valley glacier and the San Juan Mountain ice cap, Colorado. Geology 35, 739–742.
Hallet, B., Putkonen, J.K., 1994. Surface dating of dynamic landforms: young boulders on aging moraines. Science 265, 937–940.
Hardy, C.T., Muessig, S., 1952. Glaciation and drainage changes in the Fish Lake Plateau. Geological Society of America Bulletin 63, 1109–1116.
Hostetler, S.W., Giorgi, F., Bates, G.T., Bartlein, P.J., 1994. Lake-atmosphere feedbacks associated with paleolakes Bonneville and Lahontan. Science 4, 665–668.
Jewell, P.W., 2007. Morphology and paleoclimate significance of Pleistocene Lake Bonneville spits. Quaternary Research 68, 421–430.
Jones, N., Quick, A., Rupper, S., Todd, C., Koppes, M., Tingey, D., 2009. Reconstructing regional glacial and climate histories of the Sevier and Wasatch Plateaus of central Utah. Geological Society of America Abstracts with Programs 41 (6), 13.
Kurz, M.D., 1986. In-situ production of terrestrial cosmogenic helium and some applications to geochronology. Geochimica et Cosmochimica Acta 50, 2855–2862.
Kutzbach, J., Gallimore, R., Harrison, S., Behling, P., Selin, R., Laarif, F., 1998. Climate and biome simulations for the past 21, 000 years. Quaternary Science Reviews 17, 473–506.
Laabs, B.J.C., Bash, E.B., Refsnider, K.A., Becker, R.A., Munroe, J.M., Mickelson, D.M., Singer, B.S., 2007. Cosmogenic surface-exposure age limits for latest-Pleistocene glaciation and paleoclimatic inferences in the American Fork Canyon, Wasatch Mountains, Utah. U.S.A. EOS, Transactions of the American Geophysical Union 88 (52) (Fall Meeting Supplement, Abstract PP33B-1274).
Laabs, B.J.C., Plummer, M.A., Mickelson, D.M., 2006. Climate during the Last Glacial Maximum in the Wasatch and southern Uinta Mountains inferred from glacier modeling. Geomorphology 75, 300–317.
Laabs, B.J.C., Refsnider, K.A., Munroe, J.S., Mickelson, D.M., Applegate, P.J., Singer, B.S., Caffee, M.W., 2009. Latest Pleistocene glacial chronology of the Uinta Mountains: support for moisture-driven asynchrony of the last deglaciation. Quaternary Science Reviews 28, 1171–1187.
Lal, D., 1991. Cosmic ray labeling of erosion surfaces: In situ production rates and erosion models. Earth and Planetary Science Letters 104, 424–439.
Leonard, E.M., 1984. Late Pleistocene equilibrium-line altitudes and modern snow accumulation patterns, San Juan Mountains, Colorado. Arctic and Alpine Research 16, 65–76.
Leonard, E.M., 1989. Climatic change in the Colorado Rocky Mountains: estimates based on modern climate at late Pleistocene equilibrium lines. Arctic and Alpine Research 21, 245–255.
Leonard, E.M., 2007. Modeled patterns of Late Pleistocene glacier inception and growth in the Southern and Central Rocky Mountains, USA: sensitivity to climate change and paleoclimatic implications. Quaternary Science Reviews 26, 2156–2166.
Licciardi, J.M., Pierce, K.L., 2008. Cosmogenic exposure-age chronologies of Pinedale and Bull Lake glaciations in greater Yellowstone and the Teton Range, USA. Quaternary Science Reviews 27, 814–831.
Licciardi, J.M., Clark, P.U., Brook, E.J., Elmore, D., Sharma, P., 2004. Variable responses of western U.S. glaciers during the last deglaciation. Geology 32, 81–84.
Lips, E.W., Marchetti, D.W., Gosse, J.C., 2005. Revised chronology of Late Pleistocene glaciers, Wasatch Mountains, Utah. Geological Society of America Abstracts with Programs 37 (7), 41.
Locke, W.W., 1989. Present climate and glaciation of western Montana, USA. Arctic and Alpine Research 21, 234–244.
Locke, W.W., 1995. Modeling of icecap glaciations of the northern Rocky Mountains of Montana. Geomorphology 14, 123–130.
Ludwig, K.R., 1996. ISOPLOT—a plotting and regression program for radiogenic isotope data. USGS Open-File Report 91-445. 47 pp.
Marchetti, D.W., 2007. Pleistocene glaciations in central Utah: a review. Central Utah – diverse geology of a dynamic landscape: In: Willis, G.C., Hylland, M.D., Clark, D.L., Chidsey Jr., T.C. (Eds.), Utah Geological Association Publication, 36, pp. 197–203.
Marchetti, D.W., Cerling, T.E., 2005. Cosmogenic ^{3}He exposure ages of Pleistocene debris flows and desert pavements in Capitol Reef National Park, Utah. Geomorphology 67, 423–435.
Marchetti, D.W., Cerling, T.E., Lips, E.W., 2005. A glacial chronology for the Fish Creek drainage of Boulder Mountain, Utah, USA. Quaternary Research 64, 264–271.
Marchetti, D.W., Cerling, T.E., Dohrenwend, J.C., Gallin, W., 2007. Ages and significance of glacial and mass movement deposits on the west side of Boulder Mountain, Utah, USA. Palaeogeography, Palaeoclimatology, Palaeoecology 252, 503–513.
Mattox, S.R., 1991. Petrology, age, geochemistry, and correlation of the Tertiary volcanic rocks on the Awapa Plateau, Garfield, Piute, and Wayne Counties, Utah. Utah Geological Survey Miscellaneous Publication 91-5, p. 46.
McCoy, W.D., Williams, L.D., 1985. Application of an energy-balance model to the late-Pleistocene Little Cottonwood Canyon glacier with implications regarding the paleohydrology of Lake Bonneville. In: Kay, P.A., Diaz, H.F. (Eds.), *Problems and Prospects for Predicting Great Salt Lake Levels*, Center for Public Affairs, University of Utah, Salt Lake City, pp. 9–24.
Meierding, T.C., 1982. Late Pleistocene glacial equilibrium-line altitudes in the Colorado Front Range: a comparison of methods. Quaternary Research 18, 289–310.
Mulvey, W.E., 1985. Reconstruction and interpretation of late Pleistocene equilibrium line altitudes in the Lake Bonneville region: Salt Lake City, University of Utah, M.S. thesis, 65 p.
Mulvey, W.E., Currey, D.R., Lindsay, L.M.W., 1984. Southernmost occurrence of later Pleistocene glaciation in Utah: Brian Head-Signey Peaks area, Markagunt Plateau. Encyclia 61, 97–103.
Munroe, J.S., Mickelson, D.M., 2002. Reconstruction of latest Pleistocene alpine glacier equilibrium line altitudes and paleoclimate, northern Uinta Mountains, northeastern Utah, U.S.A. Journal of Glaciology 48, 257–266.
Munroe, J.S., Laabs, B.J.C., Shakun, J.D., Singer, B.S., Mickelson, D.M., Refsnider, K., Caffee, M., 2006. Latest Pleistocene advance of alpine glaciers in the southwestern Uinta Mountains, Utah, USA: evidence for the influence of local moisture sources. Geology 34, 841–844.
Ohmura, A., Kasser, P., Funk, M., 1992. Climate at the equilibrium line of glaciers. Journal of Glaciology 38, 397–411.
Osborn, G., Bevis, K., 2001. Glaciation in the Great Basin of the western United States. Quaternary Science Reviews 20, 1377–1410.
Oviatt, C.G., 1992. Quaternary geology of the Scipio Valley area, Millard and Juab counties, Utah: Utah Geological and Mineral Survey Special Study 79, 16 p., scale 1:62, 500.
Owen, L.A., Finkel, R.C., Minnich, R., Perez, A., 2003. Extreme southern margin of Late Quaternary glaciation in North America: timing and controls. Geology 31, 729–732.
Owen, L.A., Thackray, G., Anderson, R.S., Briner, J., Kaufman, D., Roe, G., Pfeffer, W., Yi, C., 2009. Integrated research on mountain glaciers: current status, priorities and future prospects. Geomorphology 103, 158–171.
Paterson, W.S.B., 1994. The Physics of Glaciers. Pergamon Press, Oxford.
Phillips, F.M., Zreda, M.G., Gosse, J.C., Klein, J., Evenson, E.B., Hall, R.D., Chadwick, O.A., Sharma, P., 1997. Cosmogenic ^{36}Cl and ^{10}Be ages of Quaternary glacial and fluvial deposits of the Wind River Range, Wyoming. Geological Society of America Bulletin 109, 1453–1463.
Pierce, K.L., 1979. History and dynamics of glaciation in the northern Yellowstone Park area. US Geological Survey Professional Paper 729F, p. 91.
Porter, S.C., 1975. Equilibrium-line altitudes of late Quaternary glaciers in the Southern Alps, New Zealand. Quaternary Research 5, 27–47.
PRISM Climate Group, Oregon State University, http://www.prismclimate.org, last accessed July 2, 2010.
Putkonen, J.K., Swanson, T., 2003. Accuracy of cosmogenic ages for moraines. Quaternary Research 59, 255–261.
Rea, B.R., Whalley, W.B., Evans, D.J.A., Gordon, J.E., McDougall, D.A., 1998. Plateau icefields: geomorphology and dynamics. Mountain Glaciation. In: Owen, L.A. (Ed.), Quaternary Proceedings, 6. John Wiley and Sons Ltd, Chichester, pp. 35–54.
Rupper, S., Roe, G.H., Gillespie, A., 2009. Spatial patterns of glacier advance and retreat in Central Asia in the Holocene. Quaternary Research 72, 337–346.

Schaefer, J.M., Denton, G.H., Barrell, D.J.A., Ivy-Ochs, S., Kubik, P.W., Andersen, B.J., Phillips, F.M., Lowell, T.V., Schlüchter, C., 2006. Near-synchronous interhemispheric termination of the last glacial maximum in mid-latitudes. Science 312, 1510–1513.

Sharp, W.D., Ludwig, K.R., Chadwick, O.A., Amundson, R., Glaser, L.L., 2003. Dating fluvial terraces by ^{230}Th/U on pedogenic carbonate, Wind River Basin, Wyoming. Quaternary Research 59, 139–150.

Spieker, E.M., Billings, M.P., 1940. Glaciation in the Wasatch Plateau. Geological Society of America Bulletin 51, 1173–1198.

Thackray, G.D., 2008. Varied climatic and topographic influences on Late Pleistocene mountain glaciations in the western United States. Journal of Quaternary Science 23, 671–681.

Thackray, G.D., Lundeen, K.A., Borgert, J.A., 2004. Latest Pleistocene alpine glacier advances in the Sawtooth Mountains, Idaho, USA: reflections of mid latitude moisture transport at the close of the last glaciation. Geology 32, 225–228.

Thackray, G.D., Owen, L.A., Chaolu, Y., 2008. Timing and nature of late Quaternary mountain glaciation. Journal of Quaternary Science 23, 503–508.

Torsnes, I., Rye, N., Nesje, A., 1993. Modern and Little Ice Age equilibrium-line altitudes on outlet valley glaciers from Jostedalsbreen, western Norway: an evaluation of different approaches to their calculation. Arctic and Alpine Research 25, 106–116.

Wagner, J.D.M., Cole, J.E., Beck, J.W., Patchett, P.J., Henderson, G.M., Barnett, H.R., 2010. Moisture variability in the southwestern United States linked to abrupt glacial climate change. Nature Geoscience 3, 110–113.

Wannamaker, P.E., Bartley, J.M., Sheehan, A.F., Jones, C.H., Lowry, A.R., Dumitru, T.A., Ehlers, T.A., Holbrook, W.S., Farmer, G.L., Unsworth, M.J., Hall, D.B., Chapman, D.S., Okaya, D.A., John, B.E., Wolfe, J.A., 2001. Great Basin-Colorado Plateau transition in central Utah: an interface between active extension and stable interior. In: Erskine, M.C., Faulds, J.E., Bartley, J.M., Rowley, P.D. (Eds.), The geologic transition, High Plateaus to Great Basin—a symposium and field guide: Salt Lake City, Utah Geological Association, pp. 1–38.

Ward, D.W., Anderson, R.S., Briner, J.P., Guido, Z.S., 2009. Signatures of glacial erosion and retreat in the Front Range landscape: cosmogenic and numerical modeling constraints. Journal of Geophysical Research—Earth Surface 114, F01026. doi:10.1029/2008JF00105.

Williams, P.L., and Hackman, R.J., 1971. Geology, structure, and uranium deposits of the Salina quadrangle, Utah: U.S. Geological Survey Miscellaneous Geological Investigations Map I-591, scale 1:250,000.

WRCC (Western Regional Climate Center—Desert Research Institute), 2006. Utah—Monthly average temperatures. Retrieved 15 April, 2009 from http://www.wrcc.dri.edu/htmlfiles/ut/ut.avg.html.